Original Research

Endoscopic Ultrasound

OPEN

A deep learning–based system to identify originating mural layer of upper gastrointestinal submucosal tumors under EUS

Xun Li[1,2,3], Chenxia Zhang[1,2,3], Liwen Yao[1,2,3], Jun Zhang[1,2,3], Kun Zhang[4], Hui Feng[5,*], Honggang Yu[1,2,3,*]

ABSTRACT

Background and Objective: EUS is the most accurate procedure to determine the originating mural layer and subsequently select the treatment of submucosal tumors (SMTs). However, it requires superb technical and cognitive skills. In this study, we propose a system named SMT Master to determine the originating mural layer of SMTs under EUS.

Materials and Methods: We developed 3 models: deep convolutional neural network (DCNN) 1 for lesion segmentation, DCNN2 for mural layer segmentation, and DCNN3 for the originating mural layer classification. A total of 2721 EUS images from 201 patients were used to train the 3 models. We validated our model internally and externally using 283 images from 26 patients and 172 images from 26 patients, respectively. We applied 368 images from 30 patients for the man-machine contest and used 30 video clips to test the originating mural layer classification.

Results: In the originating mural layer classification task, DCNN3 achieved a classification accuracy of 84.43% and 80.68% at internal and external validations, respectively. In the video test, the accuracy was 80.00%. DCNN1 achieved Dice coefficients of 0.956 and 0.776 for lesion segmentation at internal and external validations, respectively, whereas DCNN2 achieved Dice coefficients of 0.820 and 0.740 at internal and external validations, respectively. The system achieved 90.00% accuracy in classification, which is comparable with that of EUS experts.

Conclusions: Our proposed system has the potential to solve difficulties in determining the originating mural layer of SMTs in EUS procedures, which relieves the EUS learning pressure of physicians.

Key words: Submucosal tumors; EUS; Deep learning

INTRODUCTION

Submucosal tumors (SMTs) represent a class of protruding lesions that can arise from any layer of the gastrointestinal (GI) tract wall.[1,2] Compared with computed tomography and magnetic resonance imaging,[3] EUS is considered the most accurate procedure for detecting and diagnosing SMTs owing to its unique ability to examine tumors with high proximity.[4–9] Besides, EUS is the only imaging technique that can delineate the separate histologic layers of the GI tract.[10,11]

Recently, several endoscopic techniques have been proven useful in managing SMTs. Based on the experts' opinions and published case reports, when it comes to tumors arising from mucosal and submucosal layers, the procedures that can be performed include endoscopic mucosal resection (EMR), ligation device–assisted EMR,[12–17] transparent cap-assisted EMR,[18–22] and endoscopic submucosal dissection (ESD). As for tumors originating from muscularis propria, feasible procedures include endoscopic submucosal enucleation,[23,24] ESD,[25–30] endoscopic full-thickness resection,[31,32] endoscopic submucosal tunneling dissection,[33–36] and endoscopic ligation.[37–39] Therefore, it is essential to achieve an accurate identification of the originating mural layer of SMTs to select the endoscopic treatment.

However, EUS is an operator-dependent, technically challenging procedure that requires unique technical and cognitive skills. The accuracy of EUS in identifying mural layers among different endoscopists has been reported to range from approximately 59% to 94%.[40–50] This varying ability of endoscopists to distinguish mural layers leads to frequent distractors of the follow-up clinical decision, seriously impacting the effect of diagnosis and treatment. Ideally, a computer-aided mural layer annotation system could improve the ability of ultrasonic endoscopists to define the originating mural layer in SMTs.

Recent years brought a tremendous advancement of artificial intelligence (AI) in the medical field.[51] AI and EUS have been successfully combined for the identification of SMTs, and the feasibility of AI-assisted diagnosis of SMTs on ultrasound images has been preliminarily confirmed. However, these studies have been limited to the nature of SMTs and did not involve the recognition of mural

X. L., C. Z., and L. Y. contributed equally to this work.

[1] Department of Gastroenterology, Renmin Hospital of Wuhan University, Wuhan, Hubei Province, China; [2] Key Laboratory of Hubei Province for Digestive System Disease, Renmin Hospital of Wuhan University, Wuhan, Hubei Province, China; [3] Hubei Provincial Clinical Research Center for Digestive Disease Minimally Invasive Incision, Renmin Hospital of Wuhan University, Wuhan, Hubei Province, China; [4] Wuhan Union Hospital, Huazhong University of Science and Technology, Wuhan, Hubei Province, China; [5] Information center, Renmin Hospital of Wuhan University, Wuhan, Hubei Province, China.

* **Address for correspondence:** Department of Gastroenterology, Renmin Hospital of Wuhan University, 99 Zhangzhidong Road, Wuhan 430060, Hubei Province, China, Wuhan, Hubei Province, China. E-mail: fenghui7@whu.edu.cn (H. Yu); Information Center, Renmin Hospital of Wuhan University. E-mail: yuhonggang1968@163.com (H. Feng).

Supplemental digital content is available for this article. Direct URL citations are provided in the HTML and PDF versions of this article on the journal's Web site (www.eusjournal.com).

Endoscopic Ultrasound (2023) 12:6

Received: 12 April 2023; **Accepted:** 9 October 2022
Published online: 22 December 2023

http://dx.doi.org/10.1097/eus.0000000000000029

layers.[52–54] Selecting follow-up endoscopic treatment methods for SMTs is still an unsolved challenge.

In this work, we constructed a deep learning–based system, called SMT Master, to annotate mural layers and identify the originating layer of upper GI SMTs under EUS. This system was evaluated with internal and external validations on images and subsequently compared with the performance of EUS endoscopists. To the best of our knowledge, this is the first study using deep learning to distinguish mural layers and achieve mucosal visualization and the first study to define the originating mural layer of SMTs. It could be a valuable assistance in the diagnosis and treatment of SMTs and relieve the learning pressure of ultrasonic endoscopists.

MATERIALS AND METHODS

System framework

We included 3 deep convolutional neural network (DCNNs) models into the SMT Master system to achieve 2 main functions. The first was the segmentation module, which could annotate the regions of the lesions and the mural layers adjacent to them and contained 2 DCNN models: DCNN1 to segment SMTs and DCNN2 to segment the mural layers of the upper GI tract wall. The second was the classification module, DCNN3, to output and classify the originating mural layer of the observed SMTs.

Two models of the first function, especially DCNN2, were constructed to enhance the performance of the classification model, DCNN3. In particular, after the original EUS images went through DCNN1 and DCNN2, the system edited the EUS images centered on the lesion. It made 2 tangents of the lesion starting from the central point of the EUS image in white and extending for 45 degrees to the left and right sides, separately, to make 2 auxiliary lines in red (Supplementary Figure S1, http://links.lww.com/ENUS/A344). Finally, the EUS images with labeling of the lesions and mural layers within a certain range around the lesions were provided as input to DCNN3. Based on the marker information of the previous module, DCNN3 recognized the originating mural layers of SMTs (Supplementary Figure S2, http://links.lww.com/ENUS/A345). The workflow chart of SMT Master is shown in Figure 1.

Data sets, data classification, and sample distribution

A total of 2721 images from 201 EUS procedures from Wuhan Renmin Hospital during January 2019 to June 2021 were used to train the 3 models (DCNN1–3). The average age of patients was 53.8 years (SD of 11.7 years), and 69 were men (34.3%). For internal validation, 283 images from 26 EUS procedures from Renmin Hospital of Wuhan University during July 2021 to November 2021 were used. The average age was 58.0 years (SD of 10.8 years), and 11 were men (42.3%). Finally, a testing data set containing 172 images from 26 examinations of Wuhan Union Hospital was collected for external validation. The average age was 53.7 years (SD of 9.6 years), and 12 were men (46.2%). The internal and external test sets contained 97 and 69 "transition zone" images, respectively. All selected patients had previously undergone endoscopic resection, and the lesions were confirmed to be SMTs according to definite pathological findings.

Two experts were invited to mark the images, by marking the outline of the lesion and the recognizable mural layers on the lesion side. To distinguish the 5 mural layers, they marked them with different colors. Two experts classified the originating mural layer of SMT in each case according to the ESD procedure images and pathological results of the corresponding lesion. We only included EUS images from the dissenting cases if they were rediscussed by 2 experts and a unified conclusion was reached, which was then approved by 2 other experts.

All 3 models were trained and validated using the same set of images from the same group of patients. EUS images with artificial labels were used to train the DCNN1 and DCNN2 models, whereas EUS images marked by segmentation modules were used to train and test DCNN3.

A total of 368 images from 30 EUS procedures in Renmin Hospital of Wuhan University during July 2021 to December 2021 were used to compare the performance of DCNN3 with that of EUS experts (man-machine contest). The average age of the patients was 54.7 years (SD of 11.0 years), and 11 were men (36.7%). For video test, 30 video clips from 30 EUS procedures from Renmin Hospital of Wuhan University during July 2021 to November 2021 were used. The average age of patients was 56.8 years (SD of 10.8 years), and 13 were men (43.3%). These video clips included the whole process of SMT scanning, including clips before SMTs appeared in view, while scanning and after these disappeared from view; that is, there are so-called transition zones.

The sample distribution for each data set is shown in Table 1. Images from the same person were not split among the data sets. The procedures were performed using Olympus EU-ME1 and EU-ME2 (Olympus Medical Systems Co, Tokyo, Japan) processors and adapted endoscopes.

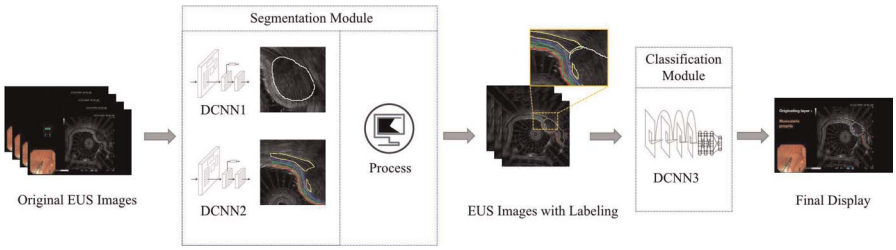

Figure 1. The framework of BP MASTER. DCNN1 was applied to segment SMTs. DCNN2 was applied to segment mural layers. DCNN was applied to classify the originating mural layers of SMTs. DCNN: deep convolutional neural network; SMT, submucosal tumor.

Table 1

Sample distribution.

	Training	Testing			
		Internal test data set	External test data set	Man-machine contest set	Video test data set
Patient (*n*)	201	26	26	30	30
Age (SD), y	53.8 (11.7)	58.0 (10.8)	53.7 (9.6)	54.7 (11.0)	56.8 (10.8)
Male, *n* (%)	69 (34.3)	11 (42.3)	12 (46.2)	11 (36.7)	13 (43.3)
Pathological diagnosis, *n* (%)					
GIST	101 (50.25)	11 (42.31)	10 (38.46)	15 (50.00)	8 (26.67)
Leiomyoma	62 (30.85)	14 (53.85)	12 (46.15)	10 (33.33)	16 (53.33)
Aberrant pancreas	22 (10.95)	0 (0.00)	0 (0.00)	3 (10.00)	2 (6.67)
Lipoma	8 (3.98)	0 (0.00)	1 (3.85)	1 (3.33)	1 (3.33)
NET	4 (1.99)	1 (3.85)	3 (11.54)	1 (3.33)	3 (10.00)
Lymphangioma	2 (0.10)	0 (0.00)	0 (0.00)	0 (0.00)	0 (0.00)
Glomus tumor	2 (0.10)	0 (0.00)	0 (0.00)	0 (0.00)	0 (0.00)
Image no.	2721	283	172	368	

SD: standard deviation, GIST: gastrointestinal stromal tumor, NET: neuroendocrine tumor.

Training of the DCNN models

We used UNet++ for image segmentation and ResNet for image classification. Both networks were trained on a NIVIDIA GeForce GTX 2080. The technical details and neural network architecture are illustrated in supplementary materials, http://links.lww.com/ENUS/A346. To train DCNN3, we used ResNet-50, which is an amateur DCNN architecture pretrained on data from ImageNet (1.28 million images from 1000 object classes). The final classification layer was replaced with another fully connected layer using transfer learning and retrained using our data sets, and the parameters were fine-tuned to fit our needs. The data set was randomly divided into 5 subsets, and each subset was individually validated with the remaining for training in Google's Tensor Flow.[55] Three methods were used to minimize the overfitting risk: dropout,[56] data augmentation,[57] and early stopping.[58] We implemented UNet++, a novel and robust architecture for medical image segmentation, for lesions and mural layers annotation to develop DCNN1 and DCNN2.[59,60] Using the original EUS image as input with the resolution of 256 × 256 and the expert-marked map as output, UNet++ was used to train and test DCNN1 and DCNN2 in an image-to-image manner in Keras. Based on the result of internal validation, we obtained the best lesion segmentation and the first to fifth mural layer segmentation thresholds by increasing 2 each time, and the threshold was set as 50, 30, 50, 30, 50, and 20 (Supplementary Figure 3, http://links.lww.com/ENUS/A347).

Man-machine contest

To evaluate the difference in the accuracy between SMT Master and endoscopists in determining the originating mural layer of SMTs, we chose 368 EUS images from 30 patients as a test data set. The endoscopists participating in this evaluation were split into 3 groups according to their experience performing EUS: 4 novices (<1 year), 3 seniors (1–3 years), and 2 experts (>3 years). Then, we asked them to carefully examine all the images and come up with a result of the SMT originating mural layer for each case. Because the choice of endoscopic treatment depended on whether SMT was located at layers 2 and 3 or layer 4, we conducted statistical analysis in 2 ways: method A, to calculate the accuracy of classifying layer 2 or layer 3, or layer 4, and method B, to estimate the accuracy of classifying layers 2 and 3 or layer 4.

Statistical analysis

To evaluate the classification of the originating mural layer, we used accuracy as a metric, which is defined as the number of correctly classified images divided by the total number of images. To evaluate the segmentation, including lesion segmentation and mural layers segmentation, intersection over union (IoU) was used, defined as the relative area of overlap between the predicted bounding box (A) and ground-truth (B) bounding box, which was labeled by the experts. IOU could be calculated as follows:

$$\mathrm{IoU} = \frac{|A \cap B|}{|A| \cup |B|}$$

If IoU>threshold, the prediction is true positive, whereas if IoU<threshold, the prediction is false positive. If the model segmentation area = 0, it is false negative. We also used the Dice coefficient, precision and recall, defined as follows, respectively:

$$\mathrm{Dice\ (F1\ score)} = \frac{2\mathrm{TP}}{2\mathrm{TP} + \mathrm{FP} + \mathrm{FN}}$$

$$\mathrm{Precision} = \frac{\mathrm{TP}}{\mathrm{TP} + \mathrm{FP}}$$

$$\mathrm{Recall} = \frac{\mathrm{TP}}{\mathrm{TP} + \mathrm{FN}}$$

Interobserver and intraobserver agreements of the endoscopists were appraised using Cohen κ coefficient. All analyses were performed using the IBM SPSS software (version 20; IBM Corp, Armonk, NY).

Human subjects

This study was approved by the Renmin Hospital Ethics Committee of Wuhan University, and the participating endoscopists provided informed consent.

Role of the funding source

The funder had no role in the study design, data collection, data analysis, data interpretation, or report writing. The corresponding author had full access to all the data in the study and was responsible for the decision to submit the work for publication.

RESULTS

Segmentation performance

The DCNN1 model achieved Dice of 0.956 in the internal testing data set, with precision and recall at 50% IoU of 92.5% and 98.9%, respectively. In the external testing data set, the Dice was 0.776, with precision and recall at 50% IoU of 67.3% and 91.7%, respectively [Table 2]. For the second, third, and fourth layers, the DCNN2 model achieved Dice values of 0.871, 0.750, and 0.840 in the internal testing data set and 0.727, 0.710, and 0.784 in the external data set, respectively [Table 3].

Classification performance

Table 4 shows the results of DCNN3 for classifying the 3 mural layers. It achieved an accuracy of 84.4% in the internal testing data set and 80.7% in the external one, and the accuracy was 80.0% in the video test. For the transition zone images in the internal and external test sets, DCNN3 achieved an accuracy of 82.5% and 81.2%, respectively. In addition, it achieved an accuracy of 80.0% when tested in the internal test set of images without mural layers marked by DCNN2, which was lower than the test set with the participation of both DCNN1 and DCNN2 (Table S1, http://links.lww.com/ENUS/A346).

Man-machine contest

Compared with the SMT Master performance, the endoscopists' performance was slightly inferior. In the testing data set for the man-machine contest, DCNN3 correctly classified the originating mural layer with an accuracy of 90.0% using both methods A and B. Meanwhile, the 2 expert, 3 senior, and 4 novice endoscopists obtained accuracy values of 83.3%, 77.8%, and 60.0% using method A and 88.3%, 84.5%, and 67.5% using method B, respectively. There were no differences among the experienced endoscopists [Table 5, Figure 2]. Thus, SMT Master showed higher accuracy than all endoscopists. The interobserver agreement between DCNN3 and the experts is shown in Table S2, http://links.lww.com/ENUS/A346.

Table 3

DCNN2 segmentation performance

	Internal test data set			External test data set		
	Dice	Precision at 50% IoU	Recall at 50% IoU	Dice	Precision at 50% IoU	Recall at 50% IoU
Layer 2	87.1	78.7	97.4	72.7	61.5	88.9
Layer 3	75.0	69.2	81.8	71.0	57.9	91.7
Layer 4	84.0	72.4	100.0	78.4	64.4	100.0
Average	82.0	73.4	93.1	74.0	61.3	93.5

All results are given as a percentage.

DCNN: deep convolutional neural network; IoU: intersection over union.

DISCUSSION

In this study, we developed an AI system named SMT Master to segment SMTs and surrounding mural layers of the upper GI tract with an excellent Dice and distinguish the originating mural layer of SMTs with high accuracy in retrospectively images and videos. We evaluated the system in both internal and external validations, and it achieved high performance. In the man-machine competition, the accuracy of SMT Master in classifying originating mural layers even exceeded the average of expert physicians. This system could serve as a valuable tool to assist the diagnosis and treatment of SMTs and reduce the pressure on EUS performers and learners.

Compared with computed tomography and magnetic resonance imaging, EUS is the first choice for the detection and diagnosis of SMTs in the upper GI tract.[61] Before treating SMTs, it is necessary to use EUS to detect the location of SMTs in the GI wall.[8] Endosonographically, the upper GI tract wall comprises 5 layers of alternating echogenicity. The first layer represents the superficial layer of the mucosa, and it is hyperechoic. The second layer constitutes the deep layer of the mucosa, including the muscularis mucosae, and it is hypoechoic. The third layer is called submucosa, and it is hyperechoic. The fourth layer is hypoechoic, called the muscularis propria, and the fifth layer is hyperechoic and called the serosa/adventitia.[62,63] By determining the location, especially the originating mural layer of SMT, EUS endoscopists can indicate the appropriate type of endoscopic resection. For example, when SMTs are limited to the muscularis mucosa or submucosa, then the standard snare polypectomy, strip biopsy, endoscopic submucosal resection with a ligation device, and endoscopic SMT resection with a transparent cap methods are valid options. On the

Table 2

DCNN1 segmentation performance.

Internal test data set			External test data set		
Dice	Precision at 50% IoU	Recall at 50% IoU	Dice	Precision at 50% IoU	Recall at 50% IoU
95.6	92.5	98.9	77.6	67.3	91.7

All results are given as a percentage.

DCNN: deep convolutional neural network; IoU: intersection over union.

Table 4

DCNN3 accuracy of classifying originating mural layer in internal and external test as well as the video test

	Internal Test	External Test	Video Test
Layer 2	87.3	80.7	77.8
Layer 3	91.6	77.3	66.7
Layer 4	81.5	81.4	86.7
Total	84.4	80.7	80.0

All results are given as a percentage.

DCNN: deep convolutional neural network.

Table 5

Performance of SMT Master and endoscopists in judging the accuracy of originating mural layer of SMTs

	SMT Master	Experts (n = 2)	Seniors (n = 3)	Novices (n = 4)
Layer 2 accuracy	83.3	83.3	77.8	70.8
Layer 3 accuracy	100.0	70.0	60.0	45.0
Layer 4 accuracy	89.5	86.8	82.5	60.5
Total accuracy in method A	90.0	83.3	77.8	60.0
Total accuracy in method B	90.0	88.3	84.5	67.5

All results are given as a percentage.

DCNN: deep convolutional neural network.

other hand, sessile SMTs that extend into the proper muscle layer can be removed by endoscopic enucleation using a snare, a cutting knife, or an insulated-tip electrosurgical knife.[5]

Although EUS is a powerful tool to diagnose SMTs, most endoscopists still cannot use it properly because of its steep learning curve and overdependence on the operator.[64] Different endoscopists have different abilities to identify mural layers, which was also reflected in the results of the man-machine competition in our study. Previous studies have reported the accuracy of EUS for the identification of mural layers to range from approximately 59% to 94%.[40–50] This is a crucial clinical problem that has negatively impacted the diagnosis and treatment of patients.

Recent years have witnessed medical integration with AI and SMT-related research using AI. Minoda et al.[54] developed a system named EUS-AI, which can make a differential diagnosis of gastrointestinal stromal tumors (GISTs) from non-GIST for subepithelial

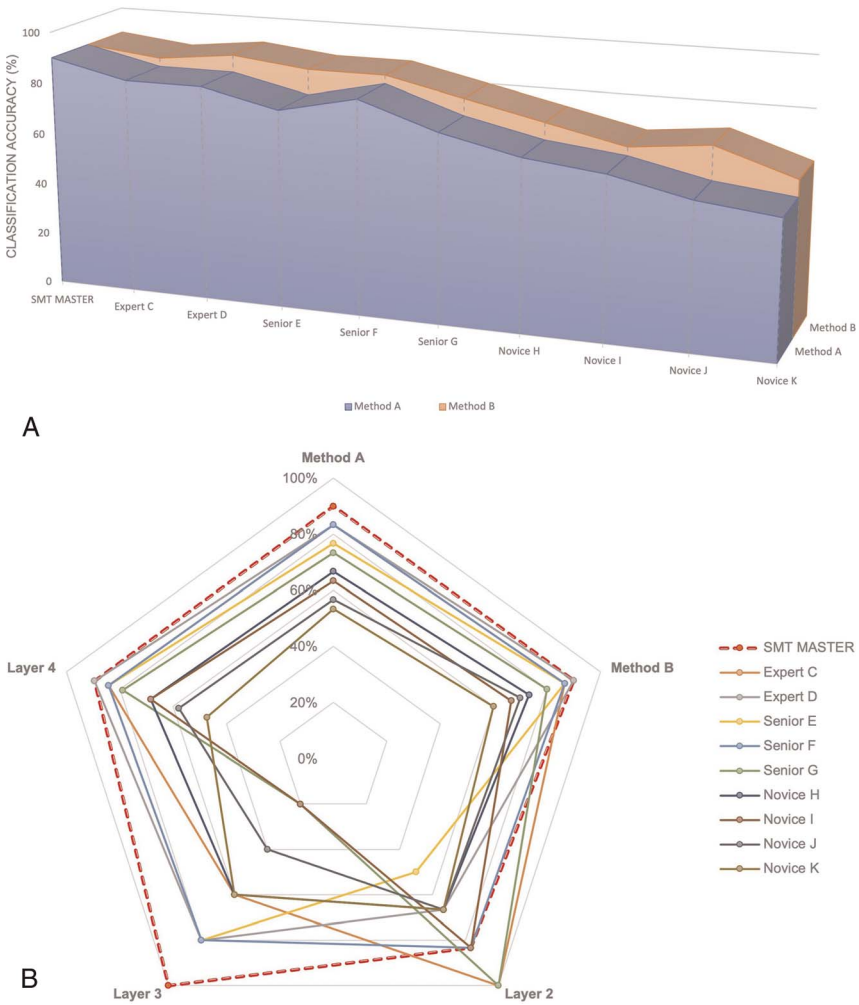

Figure 2. The accuracy in the man-machine contest. A, The accuracy of SMT Master and endoscopists of method A, method B, layer 2, layer 3, and layer 4. B, The accuracy of SMT Master and endoscopists of method A and method B. SMT, submucosal tumor

lesions ≥20 mm with an accuracy of 86.3%. The work of Seven et al.[53] reported that a deep learning algorithm could predict the malignant potential of gastric GISTs on EUS images with an accuracy of 99.6%. However, previous studies have been limited to the nature of SMTs.

In this study, we developed 2 functions: one to mark SMTs and the surrounding mural layers and one to indicate the originating mural layer. The system provides direct and indirect help for ultrasonic endoscopists to determine the location of SMTs. Endoscopists can agree with the AI's results or make other judgments based on the markers, eliminating the problem that using AI limits the physician's ability to judge. Our results showed that the accuracy of DCNN3 in classifying the EUS images with DCNN1 and DCNN2 markers was higher than that of images with only DCNN1 markers (Supplementary Figure S1, http://links.lww.com/ENUS/A344). The segmentation and labeling of mural layers by DCNN2 enhance the SMT location-related features in EUS images, thus enabling the performance of the DCNN3 classification model. Marking the local features of images first and then classifying them can overcome the existing technical bottleneck and provide a better choice for designing other medical AI schemes.

In the man-machine competition, the classification accuracy of DCNN3 was slightly higher than that of expert endoscopists (90.0% *vs.* 83.3%, respectively). Experts will generally judge the origin level of lesions according to the continuity of the mural layer, location relationship between lesions and mural layers, presence or absence of trumpet-shaped openings in the mural layer, or other features. Besides, the similar accuracy in classification to the experts implied that the model itself could also summarize the characteristics, showing the same superiority of classifying the originating mural layer of SMTs in radial EUS images. The application of SMT Master in clinical practice should be verified in prospective clinical trials in the future.

The accuracy of the external test set was not as good as the internal test. The reason might be that the parameters of the radial EUS in Wuhan Union Medical College Hospital were slightly different from ours, and the image collection style of the endoscopists in various hospitals was somewhat different, which resulted in differences in the images display. Nevertheless, SMT Master still achieved high accuracy in the external test set, which indicates that it can be applied among different hospitals.

Our study has several limitations to consider. First, although high accuracy was obtained in the external verification, the model was developed from cases and obtained at a single center. Future multicenter data collection will be necessary to enhance the generalization of our models. Second, deep learning model training using video has been proven to be practicable.[65] Although the image training–based model has achieved excellent performance in both image and video validation, the extra benefit of using video for mode training is worth to be explore in the future.

CONCLUSIONS

In conclusion, we constructed a system named SMT Master to effectively solve the problematic identification of mural layers under EUS. Our system can assist ultrasonic endoscopy physicians with the diagnosis and treatment of SMTs.

Funding

This work was supported by the Innovation Team Project of Health Commission of Hubei Province (grant no. WJ202C003) (to Honggang Yu).

Conflicts of interest

None.

Acknowledgements

The authors would like to express their gratitude to EditSprings (https://www.editsprings.cn) for the expert linguistic services provided.

Author Contributions

All authors contributed to the study conception and design. The original idea was generated by Jun Zhang and Liwen Yao. Material preparation, data collection, and analysis were performed by Xun Li, Chenxia Zhang, and Kun Zhang. The first draft of the manuscript was written by Xun Li, and all authors commented on previous versions of the manuscript. All authors read and approved the final manuscript.

References

1. Chak A. EUS in submucosal tumors. *Gastrointest Endosc* 2002;56:S43–S48.
2. Zhang J, Huang K, Ding S, et al. Clinical applicability of various treatment approaches for upper gastrointestinal submucosal tumors. *Gastroenterol Res Pract* 2016;2016:9430652–9430659.
3. Ponsaing LG, Kiss K, Loft A, Jensen LI, Hansen MB. Diagnostic procedures for submucosal tumors in the gastrointestinal tract. *World J Gastroenterol* 2007;13:3301–3310.
4. Wang J, Zhao Y, Li P, Zhang S. Advances in the application of regenerative medicine in prevention of post-endoscopic submucosal dissection for esophageal stenosis. *J Transl Int Med* 2022;10(1):28–35.
5. Shim CS, Jung IS. Endoscopic removal of submucosal tumors: preprocedure diagnosis, technical options, and results. *Endoscopy* 2005;37:646–654.
6. Hizawa K, Matsumoto T, Kouzuki T, Suekane H, Esaki M, Fujishima M. Cystic submucosal tumors in the gastrointestinal tract: endosonographic findings and endoscopic removal. *Endoscopy* 2000;32:712–714.
7. Feng L, Guo J, Wang S, et al. Endoscopic transmural drainage and necrosectomy in acute necrotizing pancreatitis: A review. *J Transl Int Med* 2021;9(3):168–176.
8. Buscarini E, Stasi MD, Rossi S, et al. Endosonographic diagnosis of submucosal upper gastrointestinal tract lesions and large fold gastropathies by catheter ultrasound probe. *Gastrointest Endosc* 1999;49:184–191.
9. Han Y, Sun S, Guo J, et al. Is endoscopic ultrasonography useful for endoscopic submucosal dissection? *Endosc Ultrasound* 2016;5:284–290.
10. Guo J, Liu Z, Sun S, et al. Endosonography-assisted diagnosis and therapy of gastrointestinal submucosal tumors. *Endosc Ultrasound* 2013;2:125–133.
11. Savoy AD, Wallace MB. EUS in the management of the patient with dysplasia in Barrett's esophagus. *J Clin Gastroenterol* 2005;39:263–267.
12. Inoue H, Endo M, Takeshita K, Yoshino K, Muraoka Y, Yoneshima H. A new simplified technique of endoscopic esophageal mucosal resection using a cap-fitted panendoscope (EMRC). *Surg Endosc* 1992;6:264–265.
13. Inoue H, Takeshita K, Hori H, Muraoka Y, Yoneshima H, Endo M. Endoscopic mucosal resection with a cap-fitted panendoscope for esophagus, stomach, and colon mucosal lesions. *Gastrointest Endosc* 1993;39:58–62.
14. Imada-Shirakata Y, Sakai M, Kajiyama T, et al. Endoscopic resection of rectal carcinoid tumors using aspiration lumpectomy. *Endoscopy* 1997;29:34–38.
15. Oshitani N, Hamasaki N, Sawa Y, et al. Endoscopic resection of small rectal carcinoid tumours using an aspiration method with a transparent overcap. *J Int Med Res* 2000;28:241–246.
16. Kajiyama T, Sakai M, Torii A, et al. Endoscopic aspiration lumpectomy of esophageal leiomyomas derived from the muscularis mucosae. *Am J Gastroenterol* 1995;90:417–422.
17. Endo S, Hirasaki S, Doi T, et al. Granular cell tumor occurring in the sigmoid colon treated by endoscopic mucosal resection using a transparent cap (EMR-C). *J Gastroenterol* 2003;38:385–389.
18. Akahoshi K, Fujimaru T, Nakanishi K, Harada N, Nawata H. Endosonography probe-guided endoscopic resection of small flat rectal carcinoid tumor using band ligation technique. *Endoscopy* 2001;33:471.

19. Ono A, Fujii T, Saito Y, et al. Endoscopic submucosal resection of rectal carcinoid tumors with a ligation device. *Gastrointest Endosc* 2003;57:583–587.
20. Niimi K, Goto O, Fujishiro M, et al. Endoscopic mucosal resection with a ligation device or endoscopic submucosal dissection for rectal carcinoid tumors: an analysis of 24 consecutive cases. *Dig Endosc* 2012;24:443–447.
21. Kim HH, Park SJ, Lee SH, et al. Efficacy of endoscopic submucosal resection with a ligation device for removing small rectal carcinoid tumor compared with endoscopic mucosal resection: analysis of 100 cases. *Dig Endosc* 2012;24:159–163.
22. Lee DG, Kim GH, Park DY, et al. Endoscopic submucosal resection of esophageal subepithelial lesions using band ligation. *Endoscopy* 2011;43:822–825.
23. Park YS, Park SW, Kim TI, et al. Endoscopic enucleation of upper-GI submucosal tumors by using an insulated-tip electrosurgical knife. *Gastrointest Endosc* 2004;59:409–415.
24. Jeong ID, Jung SW, Bang SJ, Shin JW, Park NH, Kim DH. Endoscopic enucleation for gastric subepithelial tumors originating in the muscularis propria layer. *Surg Endosc* 2011;25:468–474.
25. Lee IL, Lin PY, Tung SY, Shen CH, Wei KL, Wu CS. Endoscopic submucosal dissection for the treatment of intraluminal gastric subepithelial tumors originating from the muscularis propria layer. *Endoscopy* 2006;38:1024–1028.
26. Hwang JC, Kim JH, Kim JH, et al. Endoscopic resection for the treatment of gastric subepithelial tumors originated from the muscularis propria layer. *Hepatogastroenterology* 2009;56:1281–1296.
27. Białek A, Wiechowska-Kozłowska A, Pertkiewicz J, et al. Endoscopic submucosal dissection for treatment of gastric subepithelial tumors (with video). *Gastrointest Endosc* 2012;75:276–286.
28. Chun SY, Kim KO, Park DS, et al. Endoscopic submucosal dissection as a treatment for gastric subepithelial tumors that originate from the muscularis propria layer: a preliminary analysis of appropriate indications. *Surg Endosc* 2013;27:3271–3279.
29. Białek A, Wiechowska-Kozłowska A, Huk J. Endoscopic submucosal dissection of large gastric stromal tumor arising from muscularis propria. *Clin Gastroenterol Hepatol* 2010;8:e119–e120.
30. Liu BR, Song JT, Qu B, Wen JF, Yin JB, Liu W. Endoscopic muscularis dissection for upper gastrointestinal subepithelial tumors originating from the muscularis propria. *Surg Endosc* 2012;26:3141–3148.
31. Wang L, Ren W, Fan CQ, et al. Full-thickness endoscopic resection of nonintracavitary gastric stromal tumors: a novel approach. *Surg Endosc* 2011;25:641–647.
32. Zhou PH, Yao LQ, Qin XY, et al. Endoscopic full-thickness resection without laparoscopic assistance for gastric submucosal tumors originated from the muscularis propria. *Surg Endosc* 2011;25:2926–2931.
33. Xu MD, Cai MY, Zhou PH, et al. Submucosal tunneling endoscopic resection: a new technique for treating upper GI submucosal tumors originating from the muscularis propria layer (with videos). *Gastrointest Endosc* 2012;75:195–199.
34. Linghu E, Feng X, Wang X, Meng J, Du H, Wang H. Endoscopic submucosal tunnel dissection for large esophageal neoplastic lesions. *Endoscopy* 2013;45:60–62.
35. Khashab MA, Saxena P, Valeshabad AK, et al. Novel technique for submucosal tunneling and endoscopic resection of submucosal tumors (with video). *Gastrointest Endosc* 2013;77:646–648.
36. Ge N, Sun S, Wang S, Liu X, Wang G, Guo J. Endoscopic ultrasound-assisted tunnel-type endoscopic submucosal dissection for the treatment of esophageal tumors arising in the muscularis propria (with video). *Endosc Ultrasound* 2013;2:11–15.
37. Sun S, Jin Y, Chang G, Wang C, Li X, Wang Z. Endoscopic band ligation without electrosurgery: a new technique for excision of small upper-GI leiomyoma. *Gastrointest Endosc* 2004;60:218–222.
38. Sun S, Ge N, Wang C, Wang M, Lü Q. Endoscopic band ligation of small gastric stromal tumors and follow-up by endoscopic ultrasonography. *Surg Endosc* 2007;21:574–578.
39. Sun S, Ge N, Wang S, Liu X, Lü Q. EUS-assisted band ligation of small duodenal stromal tumors and follow-up by EUS. *Gastrointest Endosc* 2009;69:492–496.
40. Yoshinaga S, Hilmi IN, Kwek BEA, Hara K, Goda K. Current status of endoscopic ultrasound for the upper gastrointestinal tract in Asia. *Dig Endosc* 2015;27(Suppl 1):2–10.
41. Mukae M, Kobayashi K, Sada M, Yokoyama K, Koizumi W, Saegusa M. Diagnostic performance of EUS for evaluating the invasion depth of early colorectal cancers. *Gastrointest Endosc* 2015;81:682–690.
42. Murata Y, Suzuki S, Ohta M, et al. Small ultrasonic probes for determination of the depth of superficial esophageal cancer. *Gastrointest Endosc* 1996;44:23–28.
43. Hasegawa N, Niwa Y, Arisawa T, Hase S, Goto H, Hayakawa T. Preoperative staging of superficial esophageal carcinoma: comparison of an ultrasound probe and standard endoscopic ultrasonography. *Gastrointest Endosc* 1996;44:388–393.
44. Fukuda M, Hirata K, Natori H. Endoscopic ultrasonography of the esophagus. *World J Surg* 2000;24:216–226.
45. Murata Y, Napoleon B, Odegaard S. High-frequency endoscopic ultrasonography in the evaluation of superficial esophageal cancer. *Endoscopy* 2003;35: 429–35; discussion 36.
46. Esaki M, Matsumoto T, Moriyama T, et al. Probe EUS for the diagnosis of invasion depth in superficial esophageal cancer: a comparison between a jelly-filled method and a water-filled balloon method. *Gastrointest Endosc* 2006;63:389–395.
47. Goda K, Tajiri H, Ikegami M, et al. Magnifying endoscopy with narrow band imaging for predicting the invasion depth of superficial esophageal squamous cell carcinoma. *Dis Esophagus* 2009;22:453–460.
48. He LJ, Shan HB, Luo GY, et al. Endoscopic ultrasonography for staging of T1a and T1b esophageal squamous cell carcinoma. *World J Gastroenterol* 2014;20:1340–1347.
49. Jung JI, Kim GH, Hoseok I, et al. Clinicopathologic factors influencing the accuracy of EUS for superficial esophageal carcinoma. *World J Gastroenterol* 2014;20:6322–6328.
50. Lee MW, Kim GH, Hoseok I, et al. Predicting the invasion depth of esophageal squamous cell carcinoma: comparison of endoscopic ultrasonography and magnifying endoscopy. *Scand J Gastroenterol* 2014;49:853–861.
51. Torkamani A, Andersen KG, Steinhubl SR, Topol EJ. High-definition medicine. *Cell* 2017;170:828–843.
52. Hirai K, Kuwahara T, Furukawa K, et al. Artificial intelligence-based diagnosis of upper gastrointestinal subepithelial lesions on endoscopic ultrasonography images. *Gastric Cancer* 2022;25:382–391.
53. Seven G, Silahtaroglu G, Kochan K, Ince AT, Arici DS, Senturk H. Use of artificial intelligence in the prediction of malignant potential of gastric gastrointestinal stromal tumors. *Dig Dis Sci* 2022;67:273–281.
54. Minoda Y, Ihara E, Komori K, et al. Efficacy of endoscopic ultrasound with artificial intelligence for the diagnosis of gastrointestinal stromal tumors. *J Gastroenterol* 2020;55:1119–1126.
55. Abadi M, Barham P, Chen JM, et al. TensorFlow: a system for large-scale machine learning. 12th USENIX Symposium on Operating Systems Design and Implementation (OSDI); November 2–4, 2016; Savannah, GA2016.
56. Baldi P, Sadowski P. The dropout learning algorithm. *Artif Intell* 2014;210:78–122.
57. Mikolajczyk A, Grochowski M. Data augmentation for improving deep learning in image classification problem. *International Interdisciplinary Phd Workshop* 2018.
58. Duvenaud DK, Maclaurin D, Adams RP. *Early Stopping as Nonparametric Variational Inference*. Network Softwarization; 2016.
59. Deng J, Dong W, Socher R, Li LJ, Li FF. ImageNet: a large-scale hierarchical image database. 2009 IEEE Computer Society Conference on Computer Vision and Pattern Recognition (CVPR 2009), 20–25 June 2009, Miami, Florida, USA; 2009.
60. Zhou Z, Siddiquee MMR, Tajbakhsh N, Liang J. UNet++: A Nested U-Net Architecture for Medical Image Segmentation. 2018.
61. Naleschinski D, Wasner G, Rehm S, Baron R. Push-and-pull enteroscopy in the small bowel using the double-balloon technique: results of a prospective European multicenter study. *Endoscopy* 2005;37:613–616.
62. Fockens P. Current endosonographic possibilities in the upper gastrointestinal tract. *Baillieres Clin Gastroenterol* 1994;8:603–619.
63. Wiech T, Walch A, Werner M. Histopathological classification of nonneoplastic and neoplastic gastrointestinal submucosal lesions. *Endoscopy* 2005;37: 630–634.
64. Wani S, Coté GA, Keswani R, et al. Learning curves for EUS by using cumulative sum analysis: implications for American Society for Gastrointestinal Endoscopy recommendations for training. *Gastrointest Endosc* 2013;77:558–565.
65. Ouyang D, He B, Ghorbani A, et al. Video-based AI for beat-to-beat assessment of cardiac function. *Nature* 2020;580:252–256.